LASER CLADDING NICKEL BASED SUPERALLOY INCONEL 625

Dmitriy MASAYLO, Anatoliy POPOVICH, Vadim SUFIIAROV, Eugeniy BORISOV, Igor POLOZOV, Alexey ORLOV

National Technology Initiative Center of Excellence in Advanced Manufacturing Technologies at Peter the Great St. Petersburg Polytechnic University, Russian Federation, dmasaylo@gmail.com

Abstract

This paper represents the layer-by-layer synthesis results of the specimens obtained by laser cladding (LC) method. For basic material was used heat-resistant nickel alloy Inconel 625 constituting spherical shape powder. Process conditions of the LC was studied which are maintain the stable synthesis process. Structural study and mechanical test of specimens were carried out both after the manufacturing process and after the heat treatment process. Increasing of the mechanical characteristics possibility due to high-frequency vibrations during the synthesis process was studied.

Keywords: Additive technology, laser cladding, Inconel 625

1. INTRODUCTION

The need to reduce the weight of products, save material, as well as improve the performance characteristics of products leads to an increase in the complexity of parts, and, consequently, to the technology of manufacturing similar products [1-4].

Traditionally, for the manufacture of products of complex configuration, foundry technologies or machining were used. But these methods have a number of limitations, and, often, are not economically profitable. The development of industry requires substantial modernization of existing technologies, including the creation of new ones. Additive technologies (AT) play a special role in this.

AT or layer-by-layer synthesis technologies are currently one of the most dynamically developing promising production processes [5-6]. They provide engineers with an innovative approach to the design and manufacture of parts. The use of AT in many cases provides greater freedom in the choice of the configuration of the product, which allows to optimize the mass and functional parameters of the part due to the use of honeycomb, cellular and other complex structures, reducing the thickness of the walls, and combining several parts and assemblies into a single design, one whole. One of the promising directions of AT is laser cladding, the principle of which is the supply of building material (powder) directly to the reflow zone [7-9].

2. MATERIALS AND METHODS OF RESEARCH

To implement the technology of laser cladding, an installation was developed that contains the following components: a cladding head, a source of laser radiation, a powder feeder and a manipulator.

The cladding head is the main working organ in a laser cladding installation that combines many systems: a laser focusing system, a cooling system, a material feeding system and control systems (sensors, cameras, etc.). Analysis of the literature data showed that the most interesting is the three-jet cladding head, which is produced in the company Fraunhofer with a coaxial supply of protective gas directly to the cladding zone. It provides processing angles of up to 900, laser radiation power up to 5 kW, and a maximum material utilization factor of up to 95%.

In accordance with the choice of the cladding head, a fiber laser LS-3 was used - the maximum power was 3 kW with a wavelength of 1070 nm.

At present, there are a lot of companies producing gas-powder mixture feeding modules on the market. All of them are built on the same principle of action: the powder is transported by a carrier gas (argon or nitrogen, depending on the deposited material). The powder feed is controlled by a rotating dosing disk. With increasing rotation speed, a larger volume of powder enters the system. As a result, a powder feeder with two flasks of the company "Plakart" was used.

As an manipulator was chosen industrial robot FanucM20i. This choice is due to its load capacity, a large number of degrees of freedom and accuracy of positioning. **Figure 1** shows the installation of laser cladding.

Figure 1 Additive installation of laser cladding

The main parameters of the cladding process are the power of laser radiation, the speed of movement of the surfacing head and the amount of powder fed.

To visualize the spatial structure of gas flows, the Schlieren method (the Tepler method) was used, which among the many other methods is the simplest, and the corresponding equipment is inexpensive and affordable (**Figure 2**). Its additional advantage is the ability to visualize weaker optical inhomogeneities.

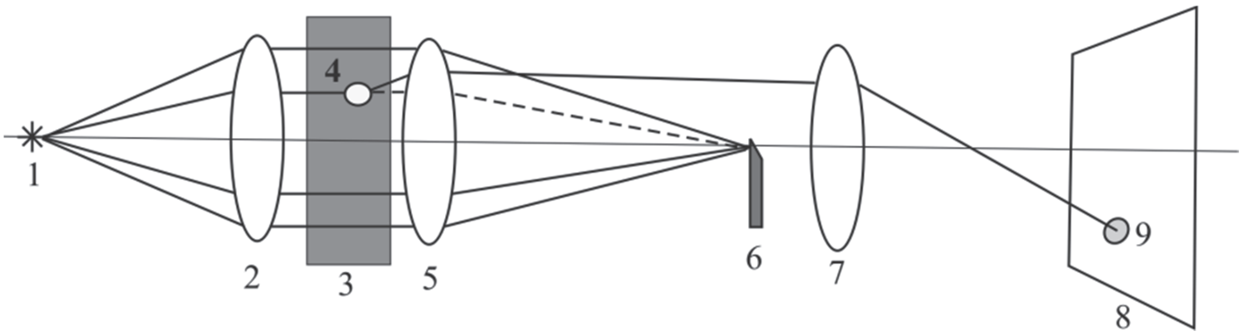

Figure 2 The essence of the Tepler method, where 1 is a point source of light; 2, 5 - the lens; 3 - the area under investigation; 4 - inhomogeneity of the refractive index of the medium; 6 - Foucault's knife; 7 - projection lens; 8 - the screen; 9 - shadow image of the inhomogeneity 4

The essence of the Tepler method is schematically represented in **Figure 2**. In its practical implementation, preference is given to systems with a parallel ray path through the investigated region, in which the decoding of shadow patterns is most simply carried out. The beam of rays from the point source of light (1), the objective of the collimator (2) is guided through the object under study (3) and is focused by the camera lens (5) on the opaque screen (6) with a sharp edge (Foucault knife), so that the source image is projected on the edge of the knife. If there are no optical inhomogeneities in the investigated object, then all the rays are delayed by the screen. In the presence of optical inhomogeneity (4), the rays will be scattered by it, and some of them, deviating, will pass above the edge of the knife. By placing the projection lens (7) behind the knife, one can build on the screen (8) an image (9) of those inhomogeneities that scattered the rays.

Visualization of powder flows was carried out using a high-speed video camera HX-4 Memrecam (Nac, USA) with a macro lens (NikkorLens AF-S VR Micro-Nikkor 105 mm). The camera provides visualization of surfacing processes with a spatial resolution of 1280 x 960 pixels and a speed of up to 6000 fps. When the resolution is reduced to 640 x 480 pixels, the shooting speed is achieved up to 23000 fps.

As the starting material, a superalloy Inconel 625 was used with a fractional composition of 45-125 µm of spherical shape (**Figure 3**).

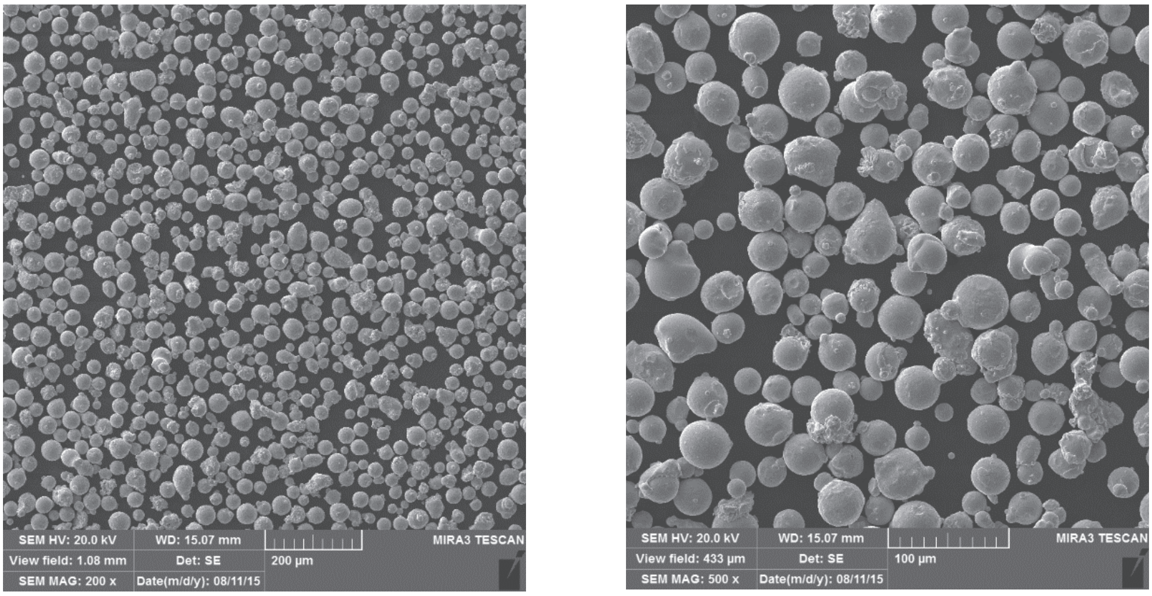

Figure 3 Photos of powder particles Inconel 625

To study the mechanical characteristics (hardness), a universal hardness tester ZwickRoell ZHU was used. The thermal treatment was carried out in argon (4N) at a temperature of 1200 °C with an exposure of 1 hour and cooling in air. Also in the work, vibration treatment was tested directly in the process of cladding [10-12]. The substrate on which the samples were grown was fixed to a vibrating table with a maximum oscillation frequency of 400 Hz.

3. RESULTS AND DISCUSSION

According to the described method, the structure of gas flows in the cladding head was studied. **Figure 4** shows the structure of the protective flow at different gas flow rates in the range from 10 to 16 l/min. **Figure 4a** shows that as the shield gas volume flow increases from 10 to 16 l/min, the length of the laminar portion of the protective gas flow is reduced. The entry of the focal point of traffic flows into the zone of turbulence of the protective flow leads to its destabilization. In addition, as shown in **Figure 4b**, excess shielding gas consumption can lead to spatial defocusing of traffic flows.

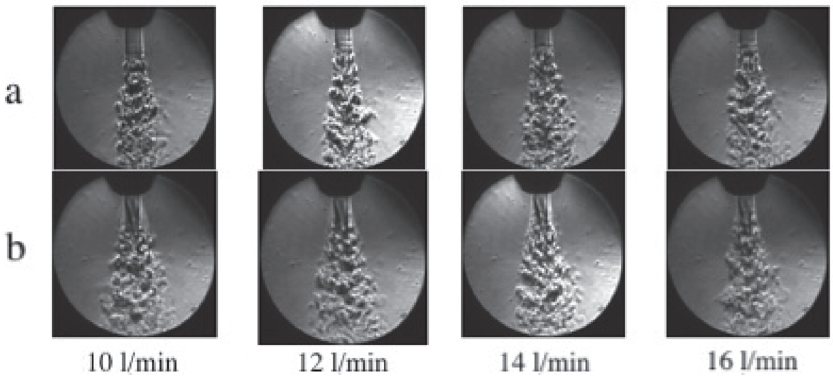

Figure 4 The scrolling images of the shielding gas flow from its volumetric flow, where a is the transport flow is absent and b - the transport flow is 3 l/min

To find the optimal ratio between the costs of shielding and transport gas, Schlieren images of gas flows in a three-jet nozzle were recorded with a variation in the protective gas flow rate in the range from 10 to 16 l/min and transport gas in the range from 1 to 5 l/min.

Figure 5a shows the Schlieren images of the flows when the volumetric flow rate of the transport gas is varied horizontally and the protective gas is used vertically. Low transport gas costs in the range from 1 to 2 l/min do not provide optimal focusing at any values of protective gas flow (from 10 to 16 l/min). The slowly moving transport stream is easily deflected by the protective flow and destabilized in its turbulent zone.

With a further increase in the transport gas flow rate up to 3 l / min, the conditions for optimal focusing are realized for a minimum protective gas flow. However, an increase in the protective gas flow rate of more than 10 l/min results in a spatial defocusing. To work with large protective flows, it is necessary to increase the transport gas consumption. In **Figure 5a**, the red lines indicate the area of optimal focusing of traffic flows. Using the obtained data it is possible, knowing the transport gas flow, to choose the appropriate value of the protective gas flow, which ensures optimal focusing.

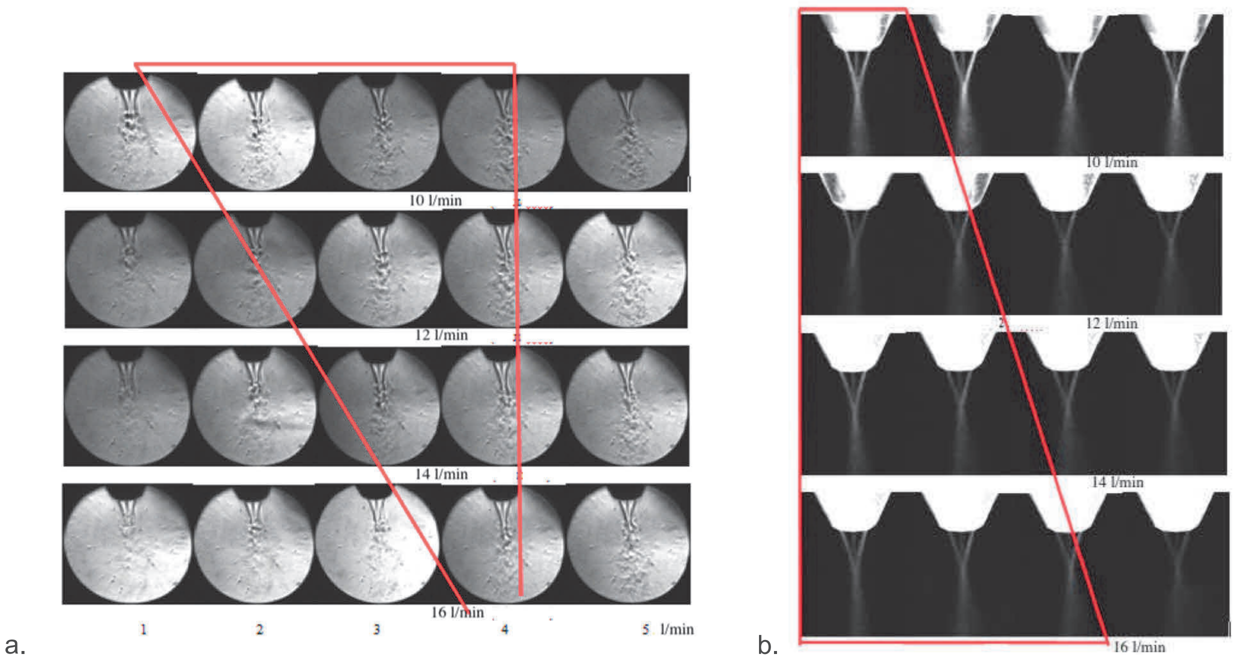

Figure 5 Optimizing the flow of shielding and transport gas in a three-jet nozzle

Figure 5b shows frames of high-speed visualization of gas-powder fluxes in a three-jet surfacing head for different values of the volumetric flow rate of protective (10-16 l/min) and transport gas (2-5 l/min). Variation of the shielding gas consumption in **Figure 5b** occurs vertically, and transport gas - horizontally. It can be seen that with a small consumption of the shielding gas, after the collision of the three powder streams, a fairly uniform distribution of particles in the plume is formed, the degree of scattering of the flow increasing with increasing transport gas flow. As the protective gas expands, the extent of the focal region increases insignificantly, and the degree of scattering of the powder decreases. The region of optimal values of transport and shielding gas flow rates, from the point of view of precision laser cladding, is shown in **Figure 5b** with a red perimeter. Within this perimeter is realized the sharpest focusing of the gas-powder flow.

The development of the laser cladding regime was carried out at a laser spot diameter of 2 mm, the distance from the substrate to the surfacing head was 12 mm, the shield gas consumption was 12 l/min, and the transport gas was 2 l/min.

During the processing of the regimes, parameters such as the laser power, the speed of the deposition of the cladding head, and the amount of the powder fed varied. **Table 1** shows the regime in which a stable process of surfacing the high-temperature Inconel 625 alloy takes place.

Table 1 Parameters of laser cladding regime for Inconel 625 (stable process)

Laser power (W)	speed (mm/s)	Amount of powder (g/min)	Speed of transport gas (l/min)	Protective gas speed (l/min)	Lifting height (mm)
1200	12	18.3	2	12	0.6

Then, according to the optimal regime, single-pass walls were made (**Figure 6**).

Figure 6 Single-pass walls of the Inconel 625 alloy

The grinds for studying the microstructure were made in two directions: along and across the growing direction. The etching of the sections was carried out in a solution of hydrochloric and nitric acid with the addition of ferric chloride. Photos of the microstructure are shown in **Figure 7**.

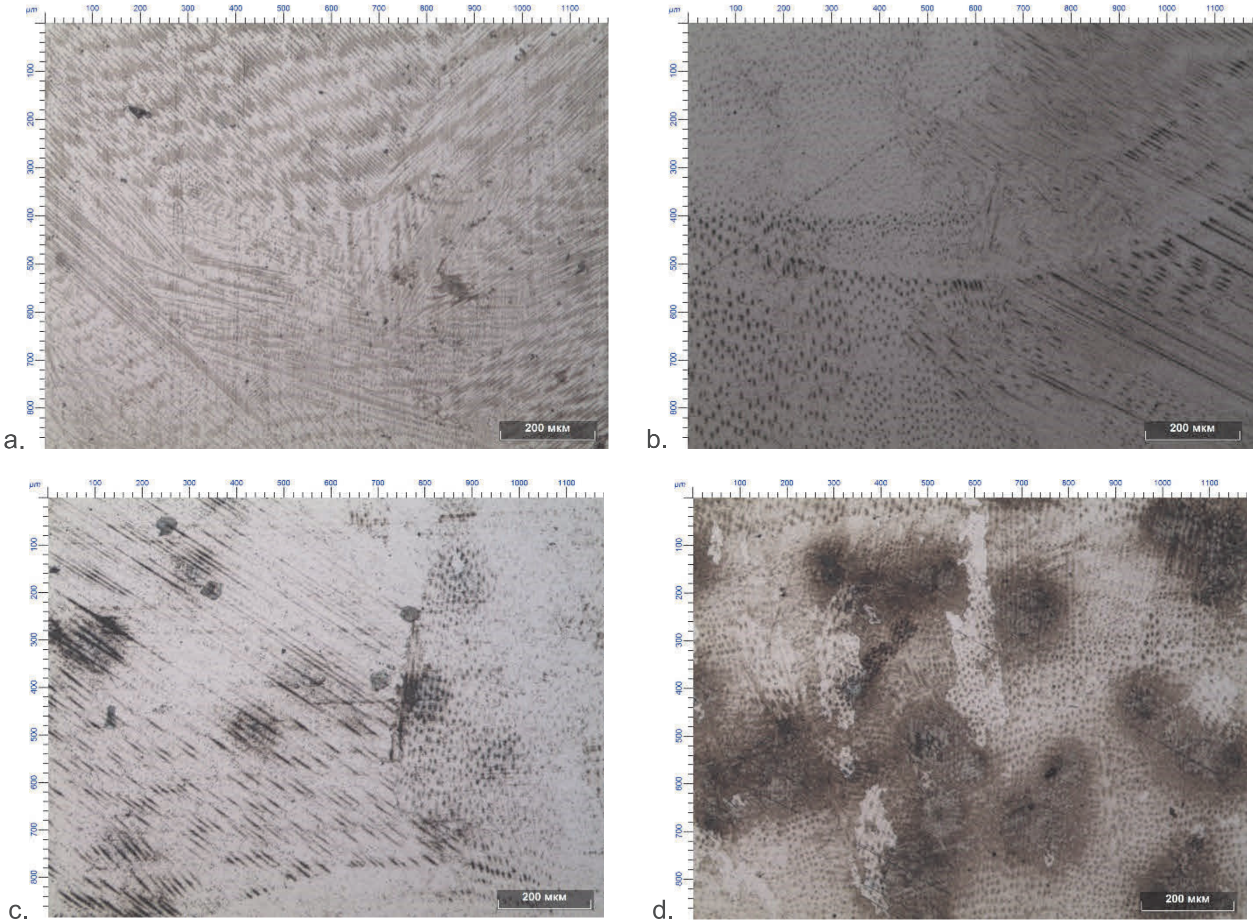

Figure 7 The microstructure images of compact samples from the Inconel 625 alloy with a magnification of 100, where: a-along the cladding direction, non-HT, b - across the cladding direction, non - HT, c - along the cladding direction, after HT, d - across the cladding of growing, after HT

On the images of the microstructures of the samples, columnar dendrites of the first, second and third kind, elongated along the cladding direction, are seen. Significant changes in the structure after heat treatment did not occur. A small enlargement of the dendrites indicates the start of the homogenization process.

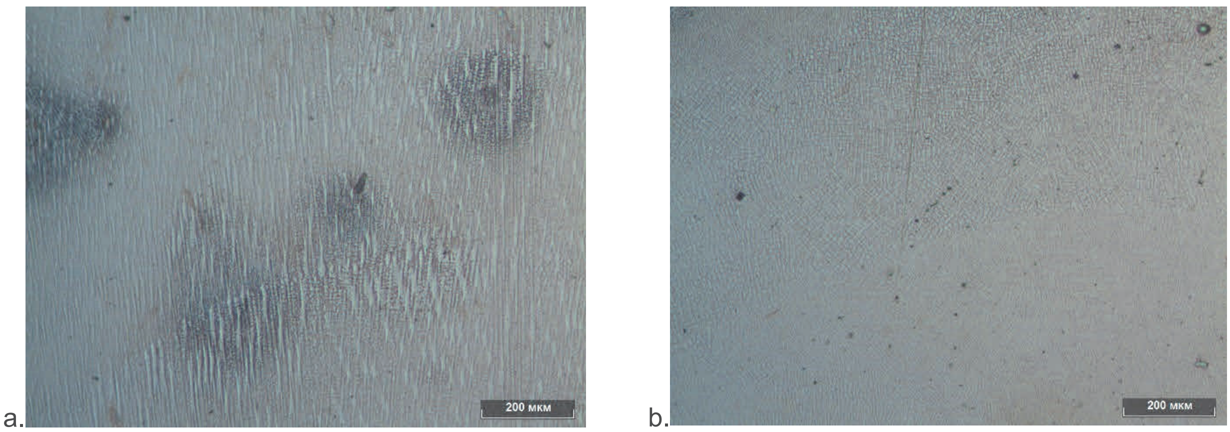

Figure 8 Images of the microstructure of compact samples from the Inconel 625 alloy with a magnification of 100 with vibration processing, where: a - is along the cladding direction, b - is across the cladding direction

The influence of vibration treatment on the structure and properties of samples was investigated. The platform was fixed on a vibration table with a frequency of oscillations of 400 Hz. A flat sample was cladding which was then sawn and pressed**. Figure 8** shows the microstructure of the resulting samples.

Analysis of the images shows that when using vibratory processing, the microstructure has become shallower, mainly dendrites of the first and second kind. Also, their quantity has significantly decreased, than when cladding without the use of vibration.

Table 2 shows the results of measuring the microhardness (Vickers method) of the obtained samples by the Vickers method.

Table 2 Results of microhardness measurements (load 10 kgs (100 N), holding time 10 s)

Sample			Sample after HT			Sample with vibration treatment		
№	HV		№	HV		№	HV	
	along	across		along	across		along	across
1	269	258	1	252	246	1	289	294
2	265	267	2	246	252	2	277	292
3	271	261	3	258	250	3	284	285
Average	268	262	Average	252	249	Average	283	290

An analysis of the results of measuring mechanical characteristics shows that heat treatment promoted the relaxation of hardening stresses. The hardness of the samples after vibration treatment increased by an average of 10% due to the formation of a finer dispersed structure.

4. CONCLUSIONS

A laser cladding unit with a three-jet feed of material to the reflow zone was developed. Modes have been developed for the stable process of obtaining samples from the superalloy Inconel 625. The microstructure before and after heat treatment - columnar dendrites of the first, second and third kind has been studied. Vibration treatment was tested in the course of laser surfacing. It is established that the microstructure of the samples is finer - dendrites of the first and second kind. Measurement of the microhardness of the samples showed that after the thermal treatment the process of stress relaxation passed. It is also established that it is possible to obtain higher mechanical characteristics by vibrating treatment - microhardness is higher by an average of 10%.

ACKNOWLEDGEMENTS

The work was carried out with the funding from the Federal Target Program «Research and Development in Priority Areas for the Development of the Russian Science and Technology Complex for 2014-2020». The unique identifier of the project RFMEFI57817X0245.

REFERENCES

[1] POPOVICH, V. A. et al. Functionally graded Inconel 718 processed by additive manufacturing: Crystallographic texture, anisotropy of microstructure and mechanical properties. *Materials & Design*. 2017. vol. 114, pp. 441-449.

[2] MUELLER, B. *Additive manufacturing technologies-Rapid prototyping to direct digital manufacturing*, Assembly Automation. 2012. T. 32, vol. 2.

[3] AHMADI, S. M. et al. Effects of heat treatment on microstructure and mechanical behaviour of additive manufactured porous Ti6Al4V. *IOP Conference Series: Materials Science and Engineering. - IOP Publishing*, 2017. vol. 293, no. 1, p. 012009.

[4] GU, D. D. et al. Laser additive manufacturing of metallic components: materials, processes and mechanisms. International Materials Reviews. 2012. vol. 57, no. 3, pp. 133-164.

[5] FRAZIER, W. E. Metal additive manufacturing: a review. *Journal of Materials Engineering and Performance*. 2014. vol. 23, no. 6, pp. 1917-1928.

[6] POPOVICH, A. et al. Producing hip implants of titanium alloys by additive manufacturing. *International Journal of Bioprinting*. 2016. vol. 2, no. 2, pp. 187-193.

[7] SEXTON, L. et al. Laser cladding of aerospace materials. *Journal of Materials Processing Technology*. 2002. vol. 122, no. 1, pp. 63-68.

[8] SHEPELEVA, L. et al. Laser cladding of turbine blades. *Surface and Coatings Technology*. 2000. vol. 125, no. 1-3, pp. 45-48.

[9] VILAR, R. Laser cladding. *Journal of Laser Applications*. 1999. vol. 11, no. 2, pp. 64-79.

[10] LANYUN, Qin, WEI, Wang and GUANG, Yang. Experimental study on laser metal deposition of FGMs with ultrasonic vibration. *Applied Mechanics and Materials*. 2012. vol. 271-272, pp. 131-135.

[11] FUDA, Ning and WEILONG, Cong. Microstructures and mechanical properties of Fe-Cr stainless steel parts fabricated by ultrasonic vibration-assisted laser engineered net shaping process. *Materials Letter*. 2016. vol. 179, pp. 61-64.

[12] XUEYONG, Chen, TODD, Sparks, JIANZHONG, Ruan and FRANK, Liou. Study of Ti64 vibration laser metal deposition process. *Advance Materials Research*. 2011. vol. 189-193, pp. 512-517.